Analysis of the Wiedemann Car Following Model over Different Speeds using Naturalistic Data

Bryan Higgs, Virginia Tech, Bryan.Higgs@vt.edu

Montasir M. Abbas, Ph.D., P.E. (Corresponding author), Virginia Tech, abbas@vt.edu

Alejandra Medina, VTTI, ale@vtti.vt.edu

ABSTRACT

This research effort analyzes the Wiedemann car-following model using car-following periods that occur at different speeds. The Wiedemann car-following model uses thresholds to define the different regimes in car following. Some of these thresholds use a speed parameter, but others rely solely upon the difference in speed between the subject vehicle and the lead vehicle. The results show that the thresholds are not constant, but vary over different speeds. Another interesting note is that the variance over the speeds appears to be driver dependent. The results indicate that the drivers exhibit different behaviors depending upon the speed which can imply an increase in aggression at particular speeds.

Keywords: Wiedemann model, Naturalistic Data, perception, reaction, model reconstruction.

BACKGROUND

The Wiedemann car-following model was originally formulated in 1974 by Rainer Wiedemann [1] . This model is known for its extensive use in the microscopic multi-modal traffic flow simulation software, VISSIM [2]. The Wiedemann model was constructed based on conceptual development and limited available data, and has to be calibrated to specific traffic stream data.

The principal ideas behind the Wiedemann model were used in this paper, but the exact shape or formula used in the model are updated using the Naturalistic Driving data that is deemed to be one of the best available sources of "real world" data [3].

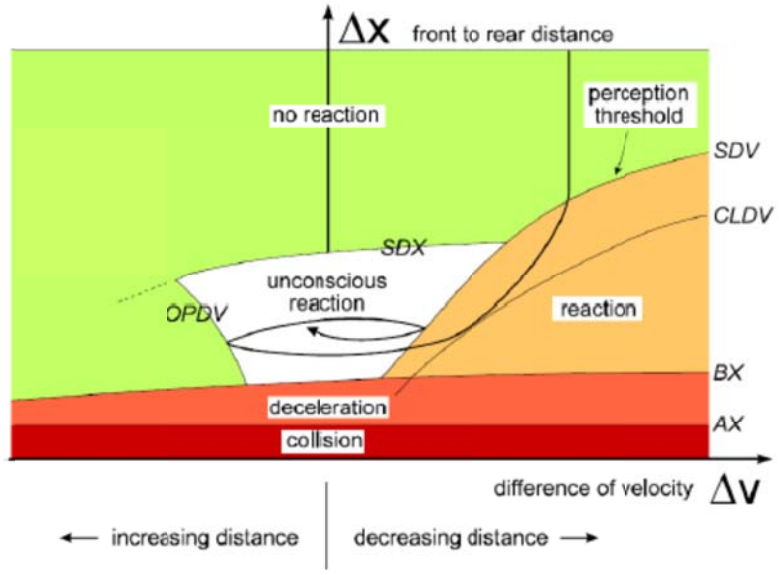

Figure 1: Wiedemann 74 Car Following Logic [2]

Figure 1 shows the graphical form of the Wiedemann 74 model. The different thresholds are shown with a certain shape that can only be amplified during the calibration procedure. The figure shows the subject vehicle approaching a lead vehicle (ΔX decreasing due to higher subject vehicle's speed shown by a positive ΔV), and entering a perception area (crossing the SDV threshold) where it has to reduce speed. The subject vehicle then crosses another threshold (CLDV) where it reacts and reduces speed even further to enter an unconscious reaction car-following episode. The subject vehicle then continues the unconscious car-following episode as long as it remains bounded by the OPDV, SDX, and SDV thresholds.

Advantages of naturalistic data

As opposed to traditional epidemiological and experimental / empirical approaches, this *in situ* process uses drivers who operate vehicles that have been equipped with specialized sensors along with processing and recording equipment. In effect, the vehicle becomes the data collection device. The drivers operate and interact with these vehicles during their normal driving routines while the data collection equipment is continuously recording numerous items of interest during the entire driving. Naturalistic data collection methods require a sophisticated network of sensor, processing, and recording systems. This system provides a diverse collection of both on-road driving and driver (participant, non-driving) data, including measures such as driver input and performance (e.g., lane position, headway, etc.), four camera video views, and driver activity data. This information may be supplemented by subjective data, such as questionnaire data.

As part of the Naturalistic Truck Driving Study DS study [3], one hundred drivers were recruited from four different trucking fleets across seven terminals and one to three trucks at each trucking fleet were instrumented (nine trucks total). After a participant finished 4 consecutive weeks of data collection, another participant started driving the instrumented truck. Three forms of data were collected by the NTDS DAS: video, dynamic performance, and audio. Approximately

14,500 driving-data hours covering 735,000 miles traveled were collected. Nine trucks were instrumented with the DAS.

The following is a typical description of how the data collection is performed, along with accompanying screen shots and information describing how the system works and how data can be used. Four cameras monitor and record the driver's face, forward road view, and left- and right-side of the tractor trailer, which are used to observe the traffic actions of other vehicles around the vehicle. Low-level infrared lighting (not visible to the driver) illuminates the vehicle cab so the driver's face and hands could be viewed via the camera during nighttime driving. The sensor data associated with the project were originally collected in a proprietary binary file format. A database schema was devised and the necessary tables were created. The schema preserves the organization of data into modules; i.e., all of the variables associated with a particular module are stored in one table in the database. The import process itself consisted of reading the binary files, writing the data to intermediate comma separated value (CSV) files and "bulk inserting" the CSV files into the database. A stored procedure is available that allows one to query the database using the module and variable names rather than database table and column names.

SYNTHESIS OF PAST EFFORTS

There have been many attempts to characterize the car-following behavior of drivers. However, direct correlation with real driving variables is rare and parameterization of objective behavior is still in its development. Some studies have been limited to very controlled experiments; recent studies have used aerial photography based measurement from helicopters [4], GPS data, test track data and trajectory data form NGSIM .

Ossen and Hoogendoorn [5] studied the car-following behavior of individual drivers using vehicle trajectory data that were extracted from high-resolution digital images collected at a high frequency from a helicopter. The analysis was performed by estimating the parameters of different specifications of the GHR car-following rule for individual drivers. In 80 % of the cases, a statistical relation between stimuli and response could be established. The Gipps (a safe distance model) and Tampere (stimulus-response model) models and a synthetic data based approach were used for assessing the impact of measurement errors on calibration results. According to the authors, the main contribution of their study was that considerable differences between the car-following behaviors of individual drivers were identified that can be expressed in terms of different optimal parameters and also as different car-following models that appear to be optimal based on the individual driver data. This is an important result taking into account that in most models a single car-following rule is used. The authors also proposed for future research to apply more advanced statistical methods and to use larger databases. Brackstone [6] using data collected with an instrumented vehicle that was assembled at TRG Southampton parameterize the Wiedemann's threshold for a typical following spiral. As a result they represent the action points as a function of a probability distribution based on ground speed.

Micro-simulation software packages use a variety of car-following models including Gipps' (AIMSUN, SISTM, and DRACULA), Wiedemann's (VISSIM), Pipe's (CORSIM), and Fritzsche's (PARAMICS). And different automated calibration parameters such as genetic algorithms have been used to calibrate the distribution of car-following sensitivity parameters *[7]*. Panwai and Dia [8] compared the car-following models between different simulation

software, including AIMSUN, PARAMICS and VISSIM using an instrumented vehicle to record differences in speed and headway (Leading speed, relative distance, relative speed, follower acceleration were recorded). The EM shows similar values for psychophysical models in VISSIM and PARAMICS and lower values in AIMSUN. The RMS error and qualitative drift and goal-seeking analyses also showed a substantially different car-following behavior for PARAMICS. Siuhi and Kaseko [9] demonstrated the need for separate models for acceleration and deceleration responses by developing a family of car-following models and addressing the shortcomings of the GM model. Previous work from Osaki [10] and Subranmanian [11] modified the GM model separating the acceleration and deceleration responses. Ahmed [12], following some work from Subranmanian assumed non linearity in the stimulus term and introduced traffic density. Results from Ahmed [12] and Toledo [13] showed , against popular belief, that acceleration increases with speed but decreases with vehicle separation. Due to statistical insignificance, Ahmed and Toledo also removed speed from their deceleration models. Siuhi and Kasvo [9] addressed some of these shortcomings by developing separate models, not only for acceleration and deceleration, but also for steady-state responses. Nonlinear regression with robust standard errors was used to estimate the model parameters and obtain the distributions across drivers. The stimulus response thresholds that delimit the acceleration and deceleration responses were determined based on signal detection theory.

Menneni et al [14] presented a calibration methodology of the VISSIM Wiedemann car-following model based on integrated use of microscopic and macroscopic data using NGSIM Relative distance vs. relative speed graphs were used for the microscopic calibration, specifically to determine the action points (it is important to note that action points were not identical to perception threshold). Scatter and distribution of action points on relative distance versus relative velocity graphs also showed similarity in driver behavior between the two freeways. Menneni also mentioned that many of the Wiedemann thresholds are velocity dependent, but a full calibration with this third dimension would be a daunting task.

Hoogendoorn and Hoogendoorn [15] proposed a generic calibration framework for joint estimation of car following models. The method employed relies on the generic form of most models and weights each model based on its complexity. This new approach can cross-compare models of varying complexity and even use multiple trajectories when individual trajectory data is scarce. Prior information can also be used to realistically estimate parameter values.

DESCRIPTION OF THE WIEDEMANN MODEL

The Wiedemann model uses random numbers in order to create heterogeneous traffic stream behavior in VISSIM. These random numbers are meant to simulate behavior of different drivers. The naturalistic data is a perfect match for this situation because the data is collected by individual drivers. Data for three different drivers was selected and processed in order to calibrate the Wiedemann car-following model. Specifically, car following periods were extracted automatically according to these conditions for each speed range:

- Radar Target ID>0

This eliminates the points in time without a radar target detected

- Radar Range<=120 meters

This represents four seconds of headway at 70 mph

- -1.9 meters<Range*Sin (Azimuth) <1.9 meters

This restricts the data to only one lane in front of the lead vehicle

- 20>=Speed>=110

This criterion would be further defined by the different speed ranges.

- Rho-inverse <=1/610 meters^{-1}

This limits the curvature of the roadway such that vehicles are not misidentified as being in the same lane as the subject vehicle when roadway curvature is present.

- Length of car following period while range is less than 61 meters >= 30 seconds

This criterion was established by trial and error as verified by video analysis.

The automatic extraction process was verified from a sample of events through video analysis. For the random sample of 400 periods, 392 were valid car following periods.

The data was divided into the following speed ranges: 20-30 kph, 30-40 kph, 40-50 kph, 50-60 kph, 60-70 kph, 70-80 kph, 80-90 kph, 90-100 kph, and 100-110 kph.

The equations that form the Wiedemann model were altered in order to remove the random parameters because they were not necessary when calibrating to a single driver. The equations shown are the altered equations which reduces the number of calibration parameters. The starting point for the Wiedemann model is the desired distance between stationary vehicles. The value calculated by Equation 1 is used in the calculations for the other thresholds.

$$\boldsymbol{AX = L_{n-1} + AXadd} \qquad (1)$$

L_{n-1} is the length of the lead vehicle

$AXadd$ is a calibrated parameter

The desired minimum following distance threshold is calculated using Equation 2 and Equation 3.

$$\boldsymbol{ABX = AX + BX} \qquad (2)$$

$$\boldsymbol{BX = BXmult} * \sqrt{\boldsymbol{v}} \qquad (3)$$

$BXmult$ is a calibration parameter

v is the minimum of the speed of the subject vehicle and the lead vehicle

The maximum following distance is calculated using Equation 4 and Equation 5.

$$\boldsymbol{SDX = AX + EX * BX} \qquad (4)$$

$$\boldsymbol{EX = EXmult} \qquad (5)$$

$EXmult$ is a calibration parameter.

The Perception Threshold marks the point that a driver will begin to react to the lead vehicle. This threshold is calculated by the use of Equation 6. Equation 1 is needed in order to calculate Equation 6.

$$\boldsymbol{SDV = \left(\frac{\Delta x - L_{n-1} - AX}{CX}\right)^2} \qquad (6)$$

L_{n-1} is the length of the lead vehicle.

CX is a calibrated parameter

The reaction curve marks the location of a second acceleration change point while still closing on the lead vehicle. In VISSIM this threshold is assumed to be equivalent to the Perception Threshold. Due to that similarity, the equation used for the Reaction Threshold, Equation 7 is derived from Equation 6.

$$\boldsymbol{CLDV = \left(\frac{\Delta x - L_{n-1} - AX}{CLDVCX}\right)^2} \qquad (7)$$

$CLDVCX$ is a calibrated parameter specific to one driver

The OPDV (Opening Difference in Velocity) curve is primarily a boundary to the unconscious reaction region. It represents the point where the driver notices that the distance between his or her vehicle and the lead vehicle is increasing over time. When this realization is made the driver will accelerate in order to maintain desired space headway. This threshold is calculated using Equation 8.

$$\boldsymbol{OPDV = CLDV * OPDVmult} \qquad (8)$$

$OPDVmult$ is a calibrated parameter

The Wiedemann model reuses the Perception Threshold as a boundary to the unconscious reaction region. This would again be the point where the driver notices that the distance between his or her vehicle and the lead vehicle is decreasing over time, but this second use of the threshold is used when the subject vehicle is already engaged in following the lead vehicle. In our representation of the model, this reuse of the Perception Threshold was given its own equation in order to separate the different uses of the threshold. Equation 9 is of the same form as Equation 6, but with a different calibrated parameter.

$$\boldsymbol{SDV2 = \left(\frac{\Delta x - L_{n-1} - AX}{CX2}\right)^2} \qquad (9)$$

$CX2$ is a calibrated parameter

The first state is the free driving regime where the subject vehicle is not reacting to a lead vehicle and is travelling at a desired speed or accelerating to a desired speed. The Free Driving Regime is defined as the area above the Perception Threshold and the Maximum Following Distance

Threshold. If the subject vehicle enters the free driving regime, the subject vehicle will then accelerate until the desired speed is reached. The value for this acceleration is calculated using Equation 10 and Equation 11. Equation 10 relates the maximum speed to the current speed times Equation 11 and calculates an acceleration value accordingly in order to reach the maximum speed.

$$\boldsymbol{b_{max} = BMAXmult * (v_{max} - v * FaktorV)} \quad (10)$$

$BMAXmult$is a calibration parameter

$v_{max}$is the maximum speed of the vehicle

$$\boldsymbol{FaktorV = FAKTORVmult} \quad (11)$$

$FAKTORVmult$ is a calibration parameter

The approaching regime occurs when a vehicle in the Free Driving Regime passes the Perception Threshold. This vehicle will then decelerate according to Equation 12.

$$\boldsymbol{b_n = \frac{1}{2}\frac{(\Delta v)^2}{ABX-(\Delta x - L_{n-1})} + b_{n-1}} \quad (12)$$

The Closely Approaching regime occurs only when a vehicle in the approaching regime passes the Closing Difference in Velocity Threshold. In VISSIM this regime is ignored, so the deceleration is still calculated by Equation 12.

The Deceleration Following regime occurs as a result of a vehicle in the Approaching or Closely Approaching regime passes the Perception Threshold or a vehicle in the Acceleration Following Regime passes the Second Perception Threshold. When a vehicle enters the Deceleration Following regime the acceleration is calculated by the negative of Equation 13.

$$\boldsymbol{b_{null} = b_{null}} \quad (13)$$

$\boldsymbol{b_{null}}$ is a calibrated parameter

The Acceleration following regime occurs when a vehicle in the Deceleration Following regime passes the Opening Difference in Velocity Threshold or a vehicle in the Emergency Regime passes the Minimum Following Distance Threshold. The acceleration for a vehicle in the Acceleration following regime is simply the positive value of Equation 13. If a vehicle in this regime accelerates and crosses the Maximum Following Distance Threshold, then that vehicle will enter the Free Driving regime. Also, the vice-versa is true where a vehicle will enter the Acceleration following regime from the Free Driving Regime if the Maximum Following Distance Threshold is passed.

The emergency regime occurs any time that the space headway is below the Minimum Following Distance Threshold. Equation 14 and Equation 15 calculate the acceleration in the Emergency regime.

$$\boldsymbol{b_n = \frac{1}{2}\frac{(\Delta v)^2}{ABX-(\Delta x - L_{n-1})} + b_{n-1} + b_{min} * \frac{ABX-(\Delta x - L_{n-1})}{BX}} \quad (14)$$

$$b_{min} = BMINadd + BMINmult * v_n \quad (15)$$

$BMINadd, BMINmult$ are calibration parameters

v_n is the speed of the subject vehicle

The adjusted equations were implemented into a calibration framework that used a genetic algorithm to calculate the optimal values of the parameters. A genetic algorithm was used because of its ability to accurately find optimal solutions that meet certain criteria when numerous parameters are present. The framework consisted of expressing the logic of the Wiedemann model as a series of state transitions. The states are defined by the different thresholds and each state has an equation or parameter for the acceleration. The optimization function was simply the minimization of the error between the velocity values calculated in the Wiedemann model and the velocity values directly from the data.

EVALUATION OF THE WIEDEMANN MODEL OVER DIFFERENT SPEED RANGES

Results of the calibration for a sample driver (Driver 49) over a different speed ranges is shown in Table 1. The length of the lead vehicle (Ln-1) shows feasible results across all of the ranges, which serves to validate the results of the calibration. The desired speed (Vdes) shows erratic behavior in the results. Vdes, FaktorVmult, and bmaxmult are all used to calculate the acceleration in the free driving regime. Judging from the variance in these parameters, the acceleration equation for the free driving regime needs to be re-evaluated.

The parameters BX and EX show smaller variance than CX, CX2, CLDVCX, and OPDV over the different speed ranges. This can be attributed to the equations that use these parameters. The equations with BX and EX include a velocity term while the other parameters have to account for the differences that speed causes. The null acceleration or bnull shows an interesting trend of high accelerations at low velocities and low acceleration at high velocities.

Table 1: Driver 49 Wiedemann Parameter Results

	20-30 kph	30-40 kph	40-50 kph	50-60 kph	60-70 kph	70-80 kph	80-90 kph	90-100 kph	100-110 kph
Ln-1	5.586	5.623	5.461	5.795	4.805	5.084	4.419	4.322	5.906
AXadd	4.540	6.941	9.611	9.152	5.613	6.230	7.899	9.187	9.890
BX	3.781	4.016	3.647	4.260	4.506	3.733	3.578	3.563	4.318
EX	2.974	3.659	3.257	3.582	3.491	2.774	2.855	3.115	3.842
CX	19.511	26.612	19.798	92.114	83.621	90.067	78.938	55.382	17.806
CX2	95.072	75.897	19.459	77.140	74.041	51.673	37.506	53.216	68.893
CLDVCX	15.518	24.870	18.487	57.298	57.721	57.315	76.277	48.422	10.000
OPDV	-3.947	-2.739	-2.299	-2.533	-2.241	-1.827	-7.024	-2.665	-5.872
bnull	0.194	0.228	0.140	0.158	0.174	0.110	0.121	0.063	0.000

bmaxmult	0.004	0.105	0.318	0.223	0.137	0.127	0.391	0.367	0.294
FaktorVmult	0.328	0.146	0.189	0.242	0.446	0.267	0.217	0.067	0.152
bminadd	-1.696	-46.706	-48.703	-47.311	-2.376	-23.471	-39.434	-18.901	-26.656
bminmult	0.283	0.332	0.124	0.081	0.085	0.336	0.319	0.170	0.247
Vdes	100.492	86.696	16.415	51.215	52.278	90.280	120.000	39.789	34.743
FaktorV	0.496	0.501	1.916	0.825	0.855	0.521	0.390	1.005	1.125
RMSE	0.905	1.067	0.863	0.821	1.177	0.639	0.807	0.719	0.576

Table 2 presents the calibration results for another driver (Driver 64) over varying speed ranges. The length of the lead vehicle (Ln-1) shows feasible values across the speed ranges which validates the calibration results. Like Driver 49's results, the BX and EX terms shows smaller variance than the other parameters. The null acceleration (bnull) reveals some interesting behavior in Driver 64 that is different from Driver 49. Remembering that bnull represents the acceleration and deceleration behavior of drivers while oscillating, the null acceleration can be used to identify when a driver has more relaxed or more aggressive acceleration and deceleration behavior while following. The higher bnull values correspond to the lower SDV2 thresholds in Table 2 with the exception on the 20-30 kph range. This means that Driver 64 has a larger following regime, graphically speaking, where the larger acceleration values exist. This correlation combines to create larger oscillation loops in the following behavior which can indicate a less attentive state than smaller oscillation loops.

Table 2: Driver 64 Wiedemann Parameter Results

	20-30 kph	30-40 kph	40-50 kph	50-60 kph	60-70 kph	70-80 kph	80-90 kph	90-100 kph	100-110 kph
Ln-1	4.123	6.000	4.305	4.151	4.172	5.407	4.133	4.322	5.016
AXadd	7.958	10.000	4.788	1.108	8.759	9.772	4.576	9.187	5.917
BX	4.678	4.250	4.406	3.175	3.770	4.666	3.152	3.563	4.224
EX	3.157	2.517	2.922	2.615	2.570	3.260	3.887	3.115	3.326
CX	94.615	71.029	48.788	19.926	32.200	88.899	90.181	55.382	65.713
CX2	70.870	81.272	43.778	100.000	45.590	36.588	70.846	53.216	54.886
CLDVCX	42.323	51.518	43.741	11.094	31.156	60.460	66.929	48.422	39.959
OPDV	-5.206	-3.484	-4.585	-3.510	-2.269	-3.395	-4.081	-2.665	-3.380
bnull	1.000	0.085	0.287	0.221	0.451	0.912	0.061	0.063	0.000
bmaxmult	0.356	0.285	0.075	0.089	0.113	0.400	0.249	0.367	0.190

FaktorVmult	0.085	0.255	0.450	0.218	0.304	0.409	0.288	0.067	0.155
bminadd	-29.008	-22.619	-9.219	-17.026	-23.879	-23.877	-11.057	-18.901	-31.202
bminmult	0.232	0.335	0.400	0.024	0.085	0.277	0.084	0.170	0.253
Vdes	18.872	35.610	74.416	28.041	99.895	57.435	12.151	90.000	57.955
FaktorV	1.936	1.089	0.679	1.305	0.490	0.795	1.982	0.462	0.725
RMSE	0.133	0.137	1.283	0.115	0.506	0.922	0.794	0.980	0.629

Table 3 presents the results of the calibration for Driver 97 over various speed ranges. Like the other two drivers' results, the BX and EX terms show smaller variance than the other parameters. The null acceleration values show a different trend than the other two drivers. The results indicate in which speed ranges the drivers will exhibit more aggressive accelerations and decelerations and also in which speed ranges the driver will exhibit more relaxed accelerations and decelerations. The results also indicate that the trends in the null acceleration across the various speed ranges are driver dependent.

Table 3: Driver 97 Wiedemann Parameter Results

	20-30 kph	30-40 kph	40-50 kph	50-60 kph	60-70 kph	70-80 kph	80-90 kph	90-100 kph	100-110 kph
Ln-1	4.747	4.112	4.743	4.076	5.052	4.986	5.701	4.806	5.054
AXadd	6.592	6.000	5.734	8.705	8.549	9.679	8.151	3.715	1.000
BX	4.389	3.342	3.581	4.788	4.998	4.774	3.122	4.101	3.275
EX	2.753	3.251	2.963	2.983	2.930	2.621	2.517	2.739	2.940
CX	48.743	48.763	27.609	46.141	59.033	55.854	45.669	44.379	74.059
CX2	27.831	80.644	60.011	44.203	58.049	26.043	59.661	45.238	94.902
CLDVCX	47.611	37.187	27.609	40.783	54.775	52.795	42.980	28.316	27.806
OPDV	-2.348	-5.076	-3.487	-2.255	-2.100	-3.838	-2.770	-4.859	-4.144
bnull	0.184	0.557	0.143	0.004	0.190	0.060	0.303	0.000	0.000
bmaxmult	0.465	0.142	0.056	0.123	0.111	0.401	0.396	0.278	0.178
FaktorVmult	0.359	0.077	0.347	0.051	0.229	0.313	0.316	0.268	0.500
bminadd	-38.648	-32.517	-23.920	-22.070	-22.940	-30.448	-13.202	-30.814	-32.488
bminmult	0.318	0.186	0.185	0.299	0.311	0.138	0.075	0.183	0.277
Vdes	12.514	35.848	32.899	53.689	57.280	87.418	27.713	102.450	78.647

FaktorV	1.787	1.106	1.131	0.755	0.750	0.551	1.266	0.467	0.674
RMSE	0.843	0.618	0.253	0.274	0.249	0.368	0.928	0.820	0.694

With a bnull value of zero or close to zero, the SDV2 and OPDV thresholds become insignificant because there is no change in acceleration or speed made when crossing either threshold. In this situation, the governing thresholds are ABX and SDX, the minimum and maximum following distance thresholds. This means that the driver will either decelerate in the emergency regime or accelerate in the free driving regime.

Table 4 presents the Root Mean Squared Error of the calibration for each Driver over the speed ranges. The values shown are all below 1.5 which suggests that the results of the calibration create a relatively low error. Table 4 also shows that the calibration within each speed range appears to be dependent on the driver.

Table 4: Root Mean Squared Error by Driver and Speed Range

	20-30 kph	30-40 kph	40-50 kph	50-60 kph	60-70 kph	70-80 kph	80-90 kph	90-100 kph	100-110 kph
Driver 49	0.9046	1.0670	0.8629	0.8207	1.1770	0.6392	0.8074	0.7186	0.5762
Driver 64	0.1331	0.1365	1.2826	0.1145	0.5063	0.9216	0.7938	0.9797	0.6291
Driver 97	0.8433	0.6181	0.2525	0.2742	0.2493	0.3677	0.9276	0.8199	0.6941

Table 5 shows the mean and standard deviation of the individual terms by driver. This table is the result of collapsing the different speed ranges in order to see the variability of each supposed constant. The results show that some of the terms have a high standard deviation while other terms have a smaller standard deviation. The terms with the lower standard deviation suggest that using a constant in their stead, as the original model suggests, would incur little error. On the other hand, using a constant in the stead of the terms with a high standard deviation would incur a large amount of error. For example, the terms CX, CX2, CLDVCX, and Vdes all have a large standard deviation which means that these terms cannot be considered a constant for the aforementioned reason.

Table 5: Average and Standard Deviation of Terms by Driver

	Average			Standard Deviation		
	Driver 49	Driver 64	Driver 97	Driver 49	Driver 64	Driver 97
Ln-1	5.22	4.63	4.81	0.591	0.687	0.497
AXadd	7.67	6.90	6.46	1.933	3.001	2.755
BX	3.93	3.99	4.04	0.353	0.594	0.730

EX	3.28	3.04	2.86	0.380	0.441	0.221
CX	53.76	62.97	50.03	32.927	26.327	12.572
CX2	61.43	61.89	55.18	23.182	20.455	22.622
CLDVCX	40.66	43.96	39.98	23.683	16.354	10.584
OPDV	-3.46	-3.62	-3.43	1.812	0.904	1.128
bnull	0.13	0.34	0.16	0.069	0.375	0.182
bmaxmult	0.22	0.24	0.24	0.133	0.125	0.150
FaktorVmult	0.23	0.25	0.27	0.111	0.132	0.140
bminadd	-28.36	-20.75	-27.45	18.489	7.456	7.595
bminmult	0.22	0.21	0.22	0.106	0.126	0.086
Vdes	65.77	52.71	54.27	34.736	31.283	30.143
FaktorV	0.85	1.05	0.94	0.475	0.580	0.419
RMSE	0.84	0.61	0.56	0.192	0.423	0.277

Figure 2 presents the AX thresholds for the three drivers over the speed ranges. The AX threshold represents the desired distance between stationary vehicles, but this value is used in the equations to calculate other thresholds and parameters. The figures show that this value is different for the speed ranges which mean that this parameter, in effect, includes some differences due to speed. This parameter should be a constant, but as the results show it is not and thus any of the equations that use this parameter will be different over the various speed ranges. This one parameter is used in the calculations for all of the thresholds and the closing deceleration.

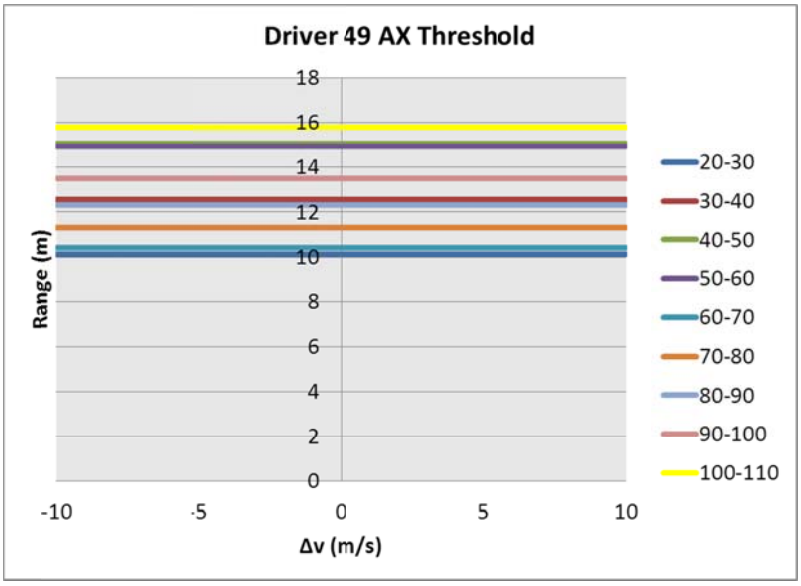

a) Driver 49 Ax Threshold

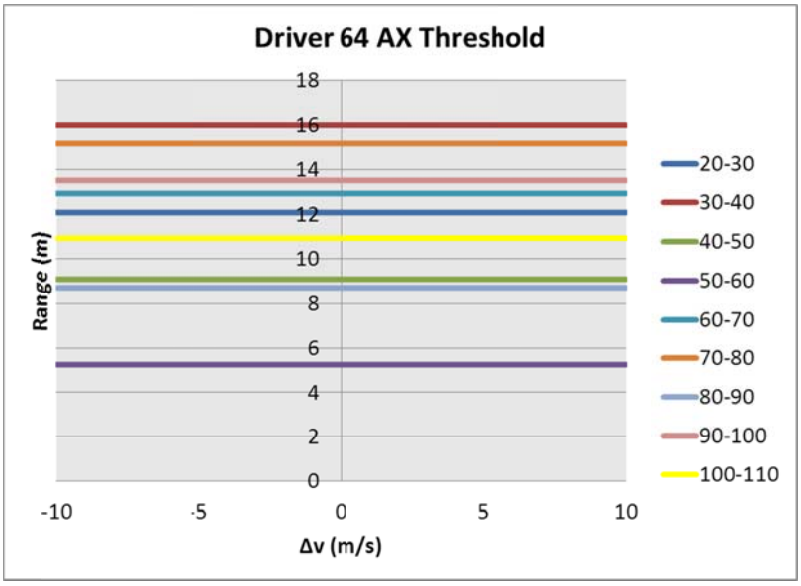

b) Driver 64 Ax Threshold

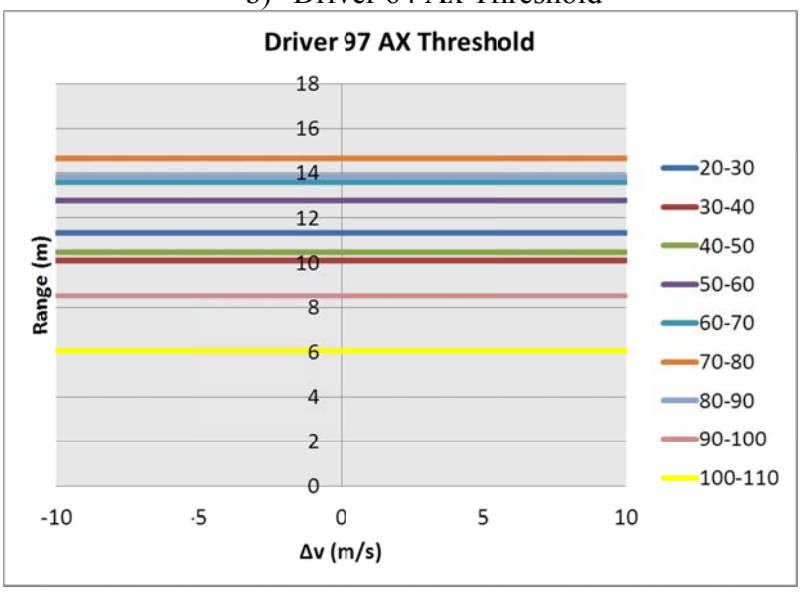

c) Driver 97 Ax Threshold

Figure 2: Driver AX Thresholds over the speed ranges

Figure 3 shows the ABX or minimum desired following distance thresholds for the three drivers. The threshold for Driver 49 shows a trend of increasing as the speed increases. The threshold for Driver 97 shows an increase as the speed increases until the 70-80 kph range then the threshold decreases as the speed increases. This indicates that the driver is more aggressive at the higher speed, speeds above 80 kph. Driver 64 shows this same aggressive behavior but in a different way. Driver 64 shows a sudden decrease in the ABX threshold from the 70-80 kph speed range to the 80-90 kph speed range, but from there, the threshold increases as the speed increases. This means that Driver 64 shows a jump in aggressiveness, but then decreasing aggression in response to higher speeds.

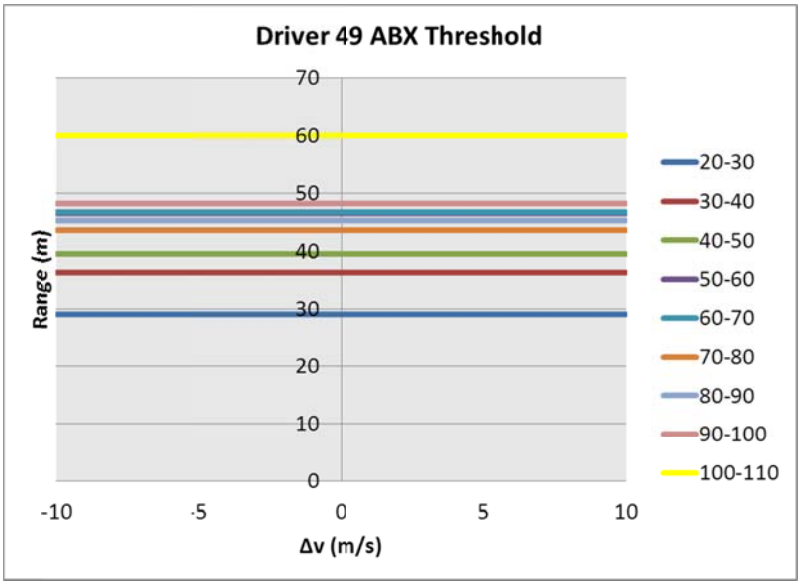

a) Driver 49 ABX Threshold

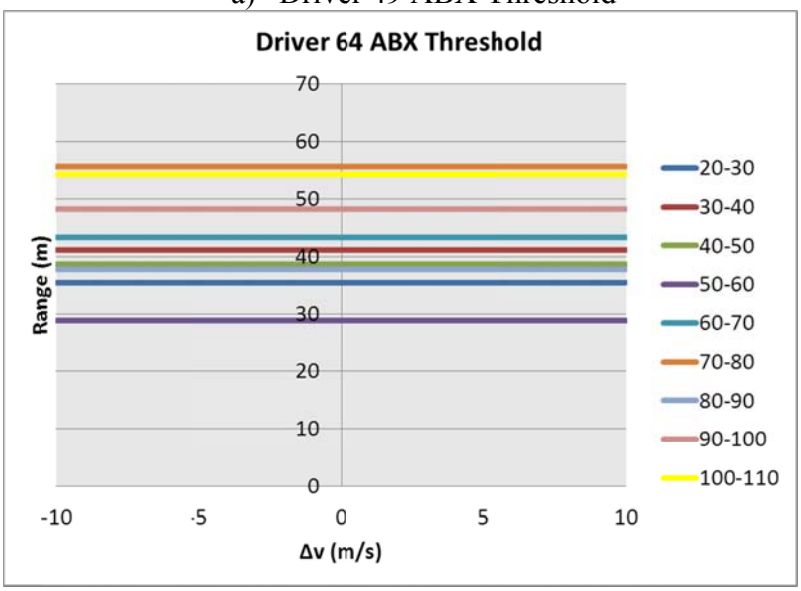

b) Driver 64 ABX Threshold

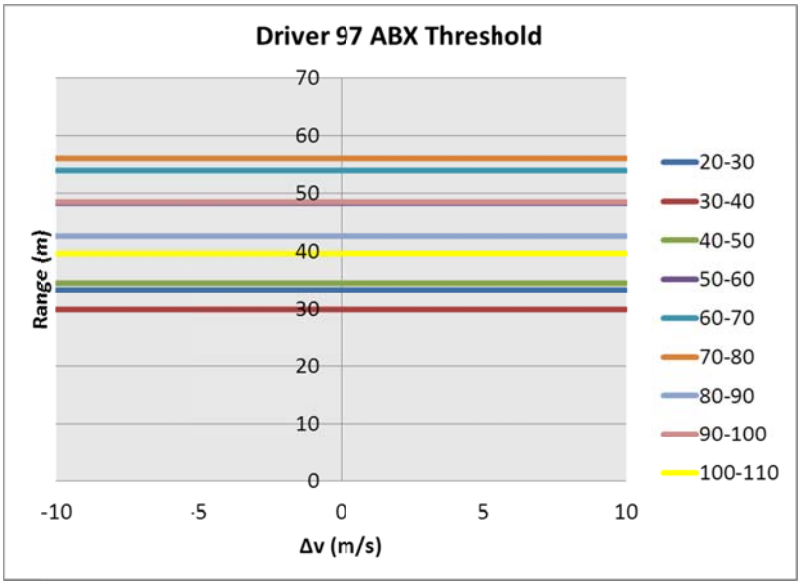

c) Driver 97 ABX Threshold

Figure 3: Driver ABX Thresholds over the speed ranges

Figure 4 shows the SDX or maximum desired following distance thresholds for the three drivers over the speed ranges. Driver 49 shows an increasing maximum desired following distance as the speeds increase up to the 60-70 kph speed range. Then, the threshold decreases by 40 meters and restarts the same increasing trend as the speed increases. The 100-110 kph threshold is far above the others which indicates that at these speeds the following regime is very large and thus the following regime can accurately represent the car following interactions. The maximum desired following distance for Driver 64 shows more of a clustering behavior than the thresholds for Driver 49. The 70-80 kph, 90-100 kph, and 100-110 kph thresholds are not included in the cluster, but these represent speeds at which Driver 64 shows car following behavior at greater distances. The maximum desired following distance for Driver 97 shows the same increase and decrease trend that was shown in the minimum desired following distance, ABX.

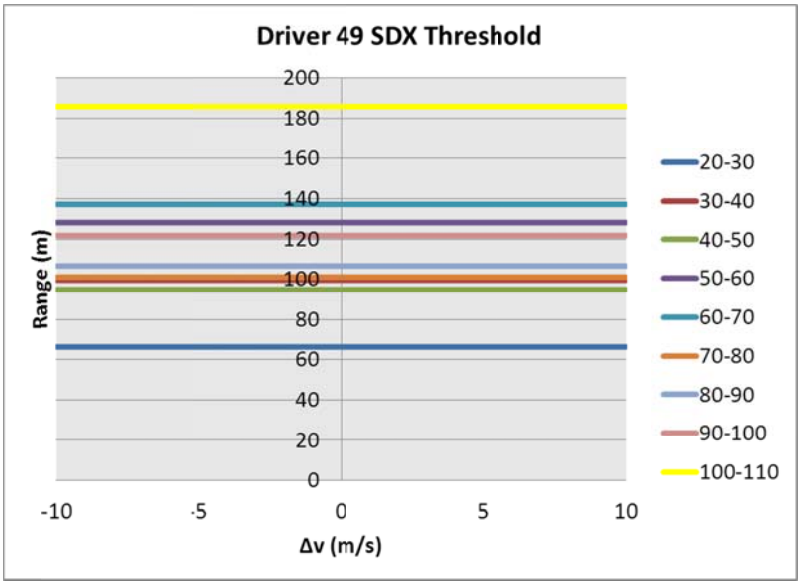

a) Driver 49 SDX Threshold

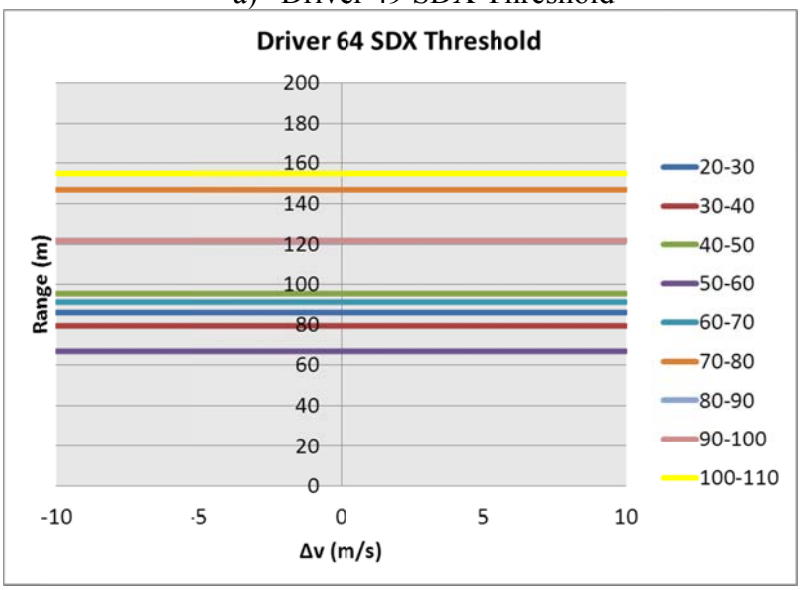

b) Driver 64 SDX Threshold

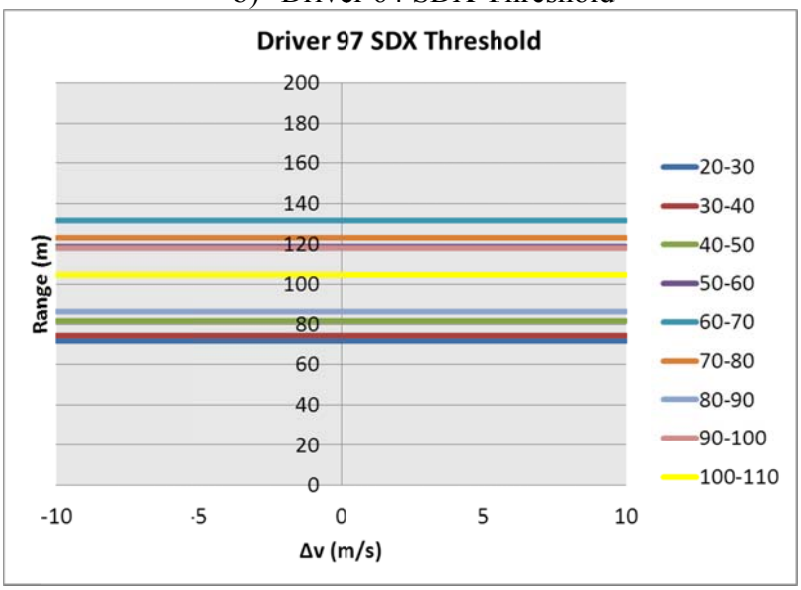

c) Driver 97 SDX Threshold

Figure 4: Driver SDX Thresholds over the speed ranges

Figure 5 shows the SDV or approaching point thresholds for the three drivers over the speed ranges. Driver 49 shows two clusters in the SDV threshold; one with speeds up to 50 kph and the second with speeds from 50 to 90 kph. Driver 64 has approaching point thresholds that begin with the lowest speed as the highest and then it decreases as the speed increases until 60 kph then it increases as the speed increases. The lower thresholds indicate that an approaching regime is not necessary at those speeds as the driver will directly enter the following regime. The thresholds in the middle indicate that an approaching regime is necessary for large speed differences, but at low speed differences, the driver will directly enter the following regime. The high thresholds indicate a necessary approaching regime except for very low speed differences.

A video reduction of a sample of the car following periods in the higher speed ranges revealed an interesting behavior in Driver 49 as compared to the other drivers. For the 100-110 kilometer per hour speed range, Driver 49 tended to approach the lead vehicles and then "settle in" and maintain that headway. This maintenance of the same headway requires Driver 49 to tap the brakes, lightly accelerate, and hold the clutch in a very active state. The 90-100 kilometer per hour speed range for Driver 49 exhibited similar behavior along with regular interaction with the lead vehicle or oscillation behavior which explains the "misplaced" SDV thresholds in Figure 5 as the two different behaviors will average out.

Driver 97, in the 100-110 kilometer per hour speed range, showed regular interaction with the lead vehicle which agrees with Figure 5. That agrees with the figure because with a higher speed and the same reaction time, the reaction distance needed will be greater for high speeds than low speeds.

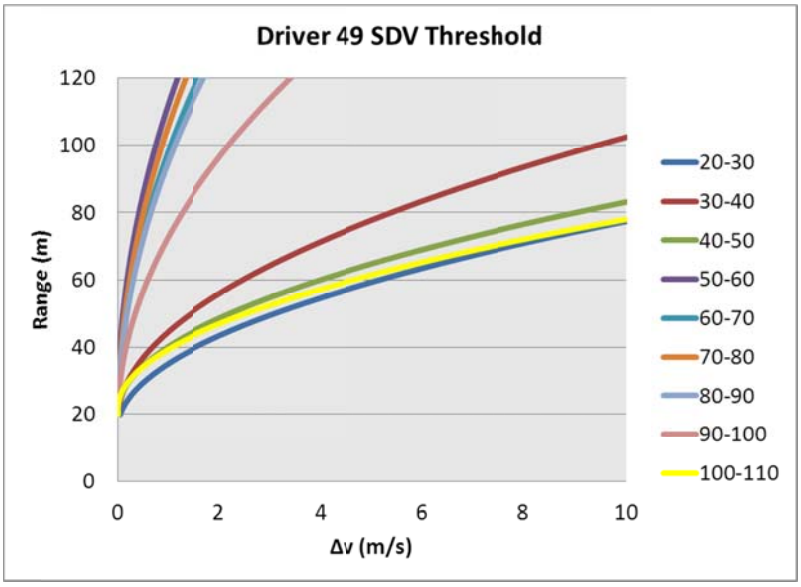

a) Driver 49 SDV Threshold

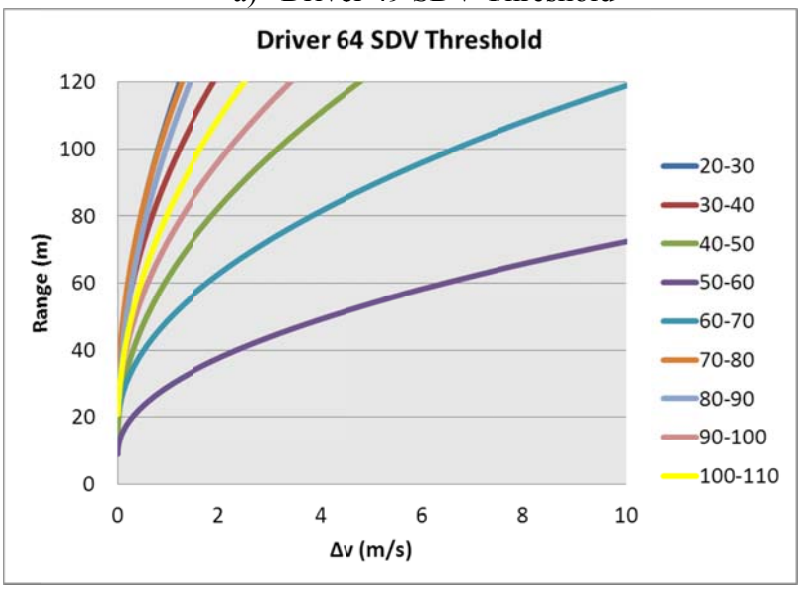

b) Driver 64 SDV Threshold

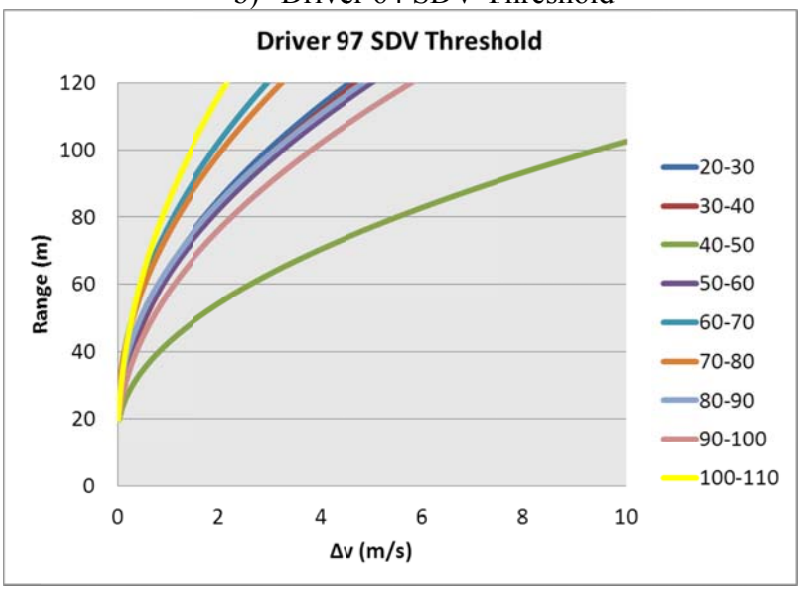

c) Driver 97 SDV Threshold

Figure 5: Driver SDV Thresholds over the speed ranges

Figure 6 shows the positive speed difference boundary or threshold to the following regime for the three drivers over the speed ranges. The thresholds for Driver 49 show two clusters; the high cluster causes a smaller following regime which indicates smaller oscillations while the lower cluster causes a larger following regime indicating larger oscillations. The speeds with larger oscillations are speeds 70-100 kph which means that at those speeds Driver 49 will wait to react until the speed difference between him and the lead vehicle is greater than at other speeds. This can almost indicate a more relaxed or distracted behavior.

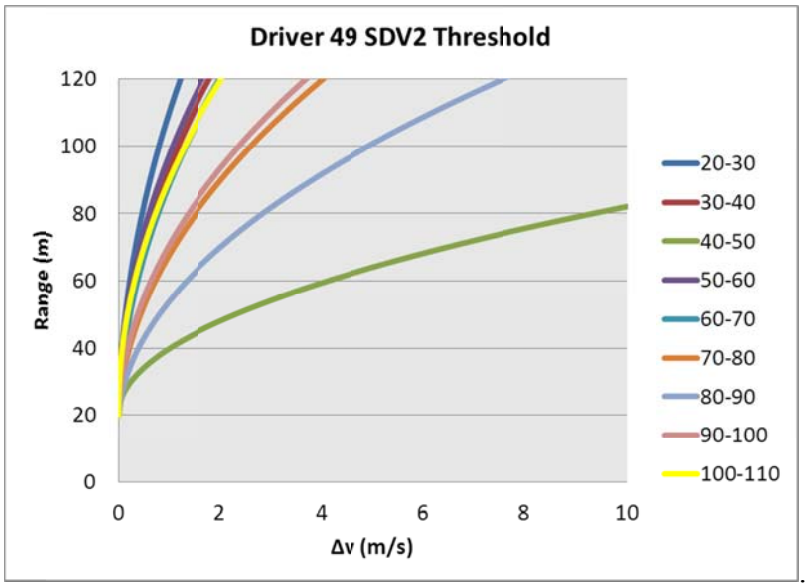

a) Driver 49 SDV2 Threshold

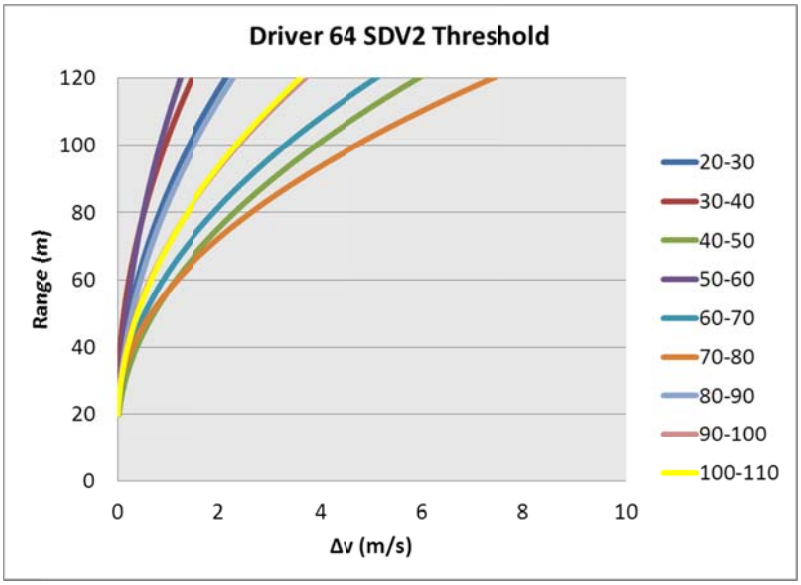

b) Driver 64 SDV2 Threshold

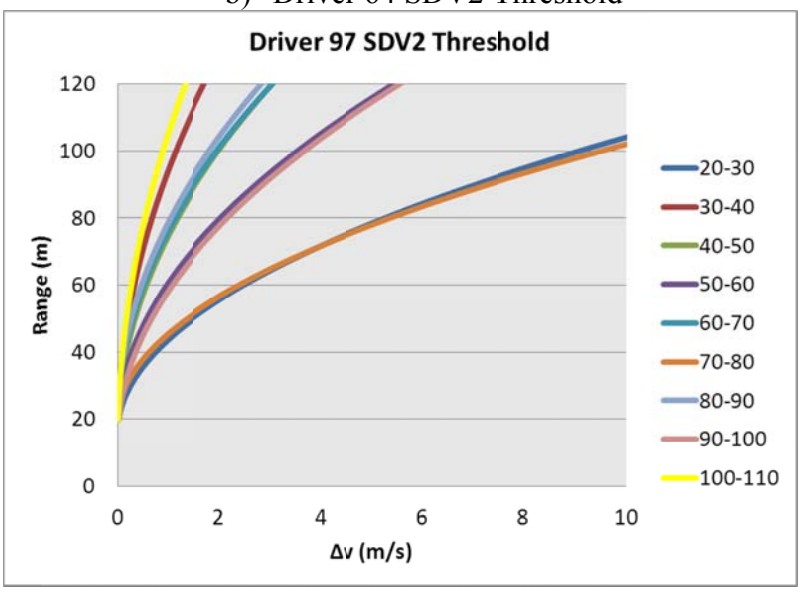

c) Driver 97 SDV2 Threshold

Figure 6: Driver SDV2 Thresholds over the speed ranges

Figure 7 presents the negative speed difference threshold (OPDV) or boundary to the following regime for the three drivers over the speed ranges. All of the thresholds in Figure 7 show a relaxed or low value as compared to the positive speed difference threshold. This shows that the drivers tend to be more responsive when approaching a lead vehicle than when falling behind a lead vehicle. Drivers 64 and 97 exhibit a clustering behavior in the OPDV thresholds, while Driver 49 shows more of a spread behavior. The OPDV thresholds for Driver 49 show an increase as the speed increases until the 70-80 kph speed range. Then, the OPDV thresholds decrease as the speed increases. The clustering of the thresholds in Driver 64 and 97 in Figure 7 indicates at which speeds the drivers are more or less responsive to falling behind the lead

vehicle. The low OPDV thresholds indicate less responsive while the high thresholds indicate more responsive behavior.

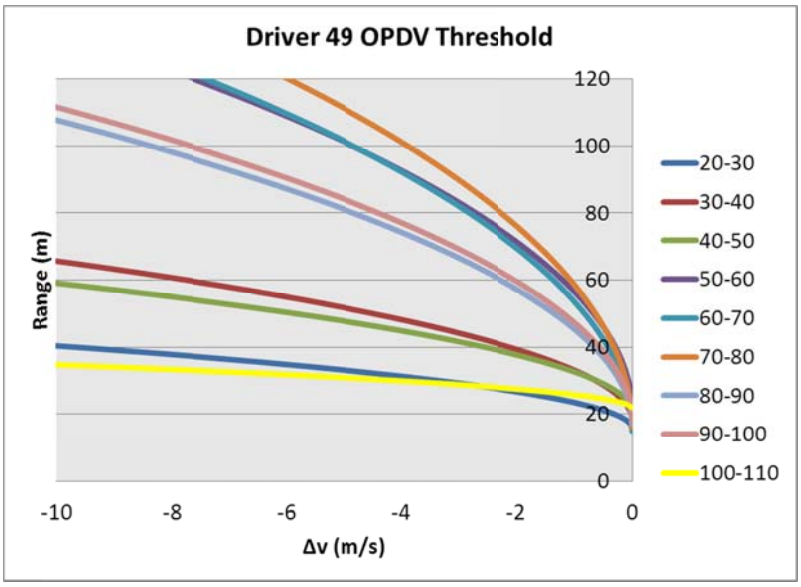

a) Driver 49 OPDV Threshold

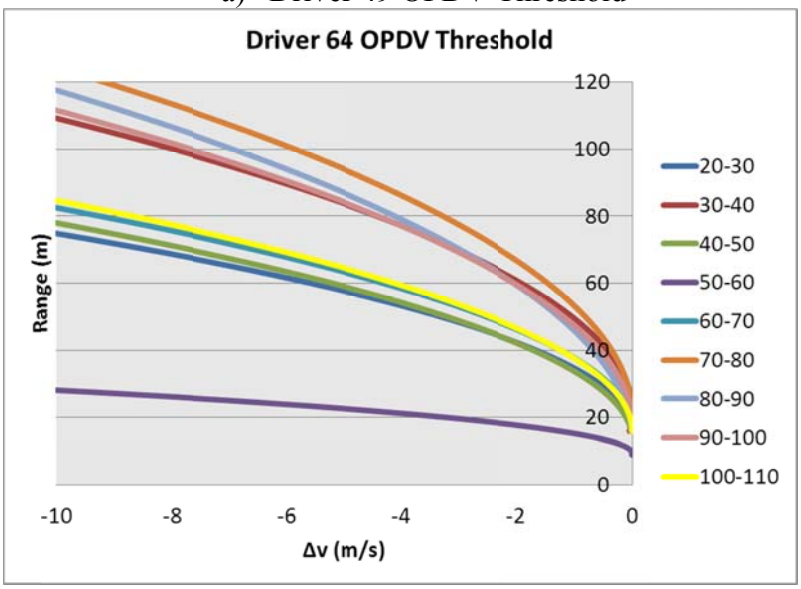

b) Driver 64 OPDV Threshold

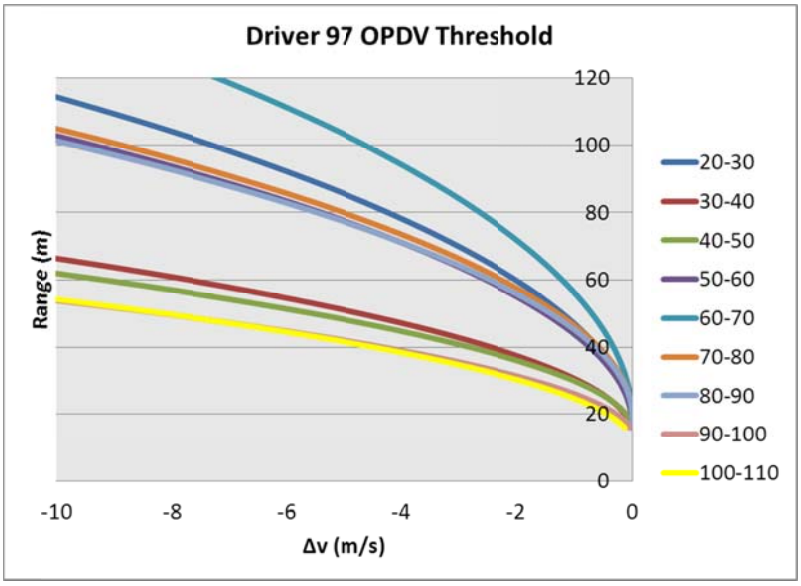

c) Driver 97 OPDV Threshold

Figure 7: Driver OPDV Thresholds over the speed ranges

CONCLUSIONS

The results show that the thresholds of the Wiedemann model vary over the speed ranges. This variation seems to be dependent upon the driver and thus driver profiles should be used instead of a single parameter. The null acceleration also shows variance over the speed ranges that seem to be driver dependent. The OPDV and SDV2 thresholds show that the drivers are more responsive to approaching than falling behind a lead vehicle. The variances also show at which speeds each driver exhibits aggressive behavior which adds value to the model. The inclusion of different aggression behavior for different speeds will only improve the Wiedemann model and make it a more realistic mimicry of the real world. As far as simulation packages are concerned, the inclusion of the ability to change the parameters according to the speed of the vehicle would serve to increase the accuracy of simulations. Future research is recommended in the development and implementation of driver aggression profiles in the Wiedemann model. Also, discovering ways to group drivers according to their profiles would potentially reduce the number of profiles needed in order to gain a more accurate simulation of traffic flow.

ACKNOWLEDGMENT

This material is based upon work supported by the Federal Highway Administration under Agreement No. DTFH61-09-H-00007. Any opinions, findings, and conclusions or recommendations expressed in this publication are those of the Author(s) and do not necessarily reflect the view of the Federal Highway Administration.

The authors would like to express thanks to Dr. C.Y. David Yang, the FHWA Agreement Manager, for his continued support and guidance during this project. They would also like to thank individuals at Virginia Tech and the Virginia Tech Transportation Institute who contributed to the study in various ways: Greg Fitch, Shane McLaughlin, Kelly Stanley and Rebecca Olson.

References

1. Wiedemann, R., *Simulation des Strassenverkehrsflusses.* Schriftenreihe des Instituts für Verkehrswesen der Universität Karlsruhe, Band 8, Karlsruhe, Germany. 1974.
2. PTV-AG, *VISSIM 5.10 User Manual.* 2008.
3. Olson, R., et al., *DRIVER DISTRACTION IN COMMERCIAL VEHICLE OPERATIONS*. 2009, Center for Truck and Bus Safety; Virginia Tech Transportation Institute: Blacksburg VA. p. 285.
4. Ranjitkar, P. and T. Nakatsuji, *A TRAJECTORY BASED ANALYSIS OF DRIVERS' RESPONSE IN CAR FOLLOWING SITUATIONS.* TRB 2010 Annual Meeting CD-ROM, 2010: p. 21.
5. Ossen, S. and S.P. Hoogendoorn, *Validity of trajectory-based calibration approach of car-following models in presence of measurement errors.* Transportation Research Record, 2008(2088): p. 117-125.
6. Brackstone, M., *Driver Psychological Types and Car Following:Is There a Correlation? Results of a Pilot Study*. 2003. p. 6.
7. Schultz, G.G. and L.R. Rilett, *Analysis of Distribution and Calibration of Car-Following Sensitivity Parameters in Microscopic Traffic Simulation Models.* 2004: p. 11.
8. Panwai, S. and H. Dia, *Comparative evaluation of microscopic car-following behavior.* IEEE TRANSACTIONS ON INTELLIGENT TRANSPORTATION SYSTEMS, 2005. **6**(3): p. 314-325.
9. Siuhi, S. and M. Kaseko, *PARAMETRIC STUDY OF STIMULUS-RESPONSE BEHAVIOR FOR CAR-FOLLOWING MODELS.* TRB 2010 Annual Meeting CD-ROM, 2010.
10. Osaki, H., *Reaction and anticipation in the Car-Following Behavior.* In Proceedings of the 12 International Symposium on the Theory of Traffic Flow and Transportation, 1993.
11. Subranmanian, H., *Estimation of Car-Following Models.* Master Thesis, 1996.
12. Ahmed, K.I., *Modeling Drivers' Acceleration and Lane Changing Behavior.* PhD Dissertation, 1999.
13. Toledo, T., *Integrating Driving Behavior.* PhD Dissertation,, 2003.
14. Menneni, S., C.P.D. Sun, P.E., and P. Vortisch, *An Integrated Microscopic and Macroscopic Calibration for Psycho-Physical Car Following Models* TRB 2009 Annual Meeting CD-ROM 2008: p. 17.
15. Hoogendoorn, S. and R. Hoogendoorn, *A Generic Calibration Framework for Joint Estimation of Car Following Models using Microscopic Data.* TRB 2010 Annual Meeting CD-ROM, 2010: p. 17.